PD-L1/PD-1 checkpoint pathway regulates hippocampal neuronal excitability and learning and memory behavior

Junli Zhao, Sangsu Bang, Kenta Furutani, Aidan McGinnis, Changyu Jiang, Alexus Roberts, Christopher R Donnelly, Qianru He, Michael L. James, Miles Berger, Mei-Chuan Ko, Haichen Wang, Richard D. Palmiter, and Ru-Rong Ji

Supplemental Information

Supplementary Figures: 1-12

Supplementary Tables: S1-S5, also see Excel files for Tables S1 and S5

Supplementary Figures and Figure Legends

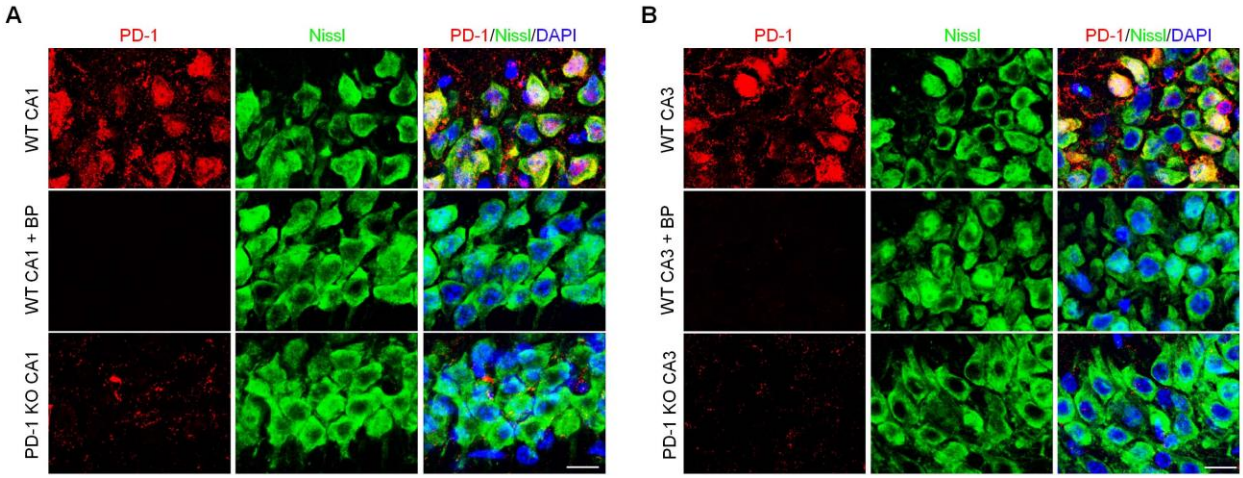

Figure S1. Characterization of PD-1 expression in mouse hippocampal neurons. Related to Figure 1.

(A) Representative images showing double immunostaining of PD-1 and Nissl in WT CA1 neurons (top) and loss of PD-1 staining after incubation with PD-1 blocking peptide in WT neurons (middle) and loss of PD-1 staining in PD-1 KO neurons (bottom). Scale bar, 20 μm.

(B) Representative images showing double immunostaining of PD-1 and Nissl in WT CA3 neurons (top) and loss of PD-1 staining after incubation with PD-1 blocking peptide in WT neurons (middle) and loss of PD-1 staining in PD-1 KO neurons (bottom). Scale bar, 20 μm.

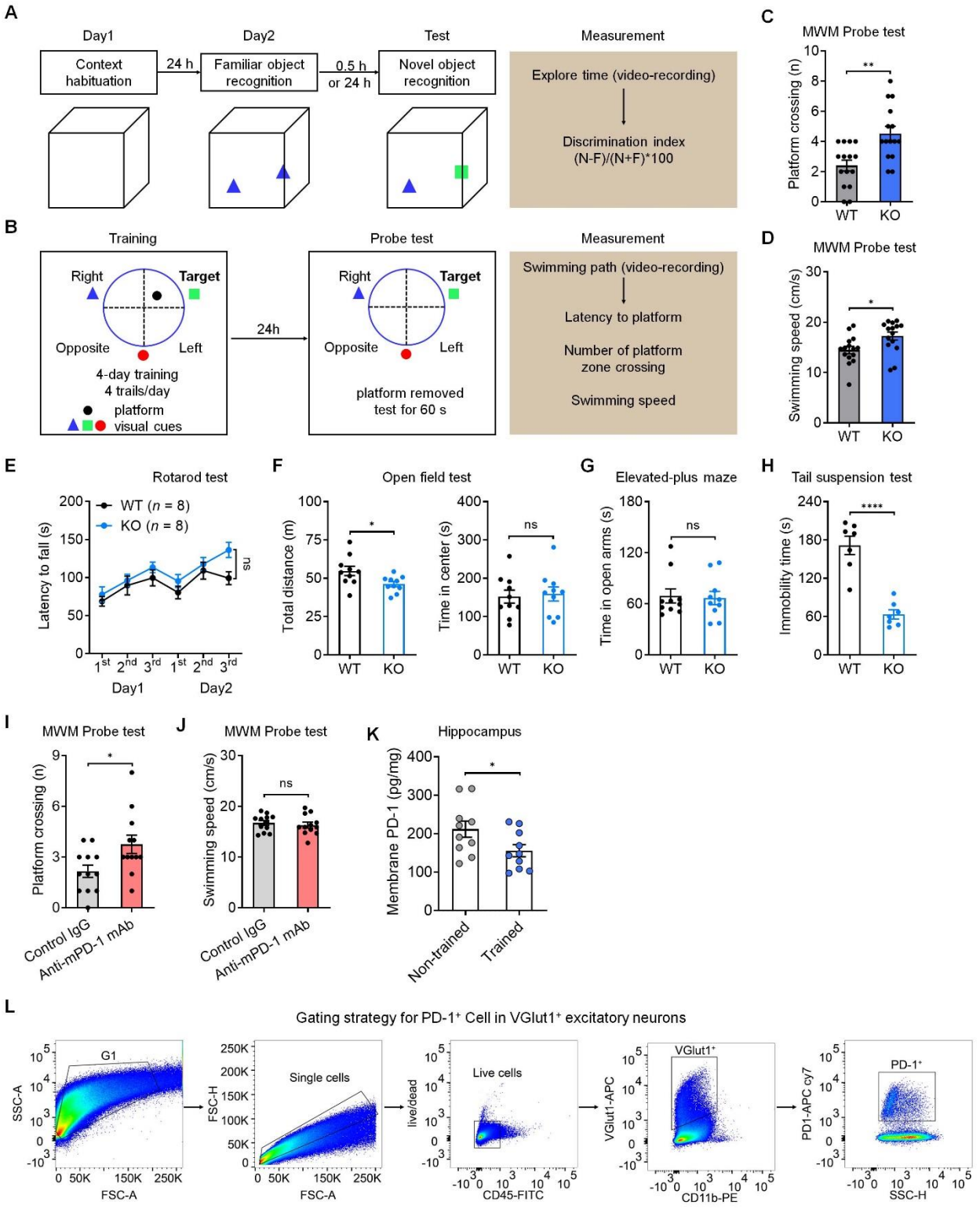

Figure S2. Characterization of learning and memory behaviors and PD-1 expression. Related to Figure 1.

(A) Schematic of NOR testing.

(B) Schematic of MWM training and probe test.

(C) MWM probe test for number of platform crossings in WT mice (n = 15) and PD-1 KO mice (n = 15).

(D) Swimming speed of WT mice (n = 15) and PD-1 KO mice (n = 15) in MWM probe tests.

(E) Motor coordination of WT mice (n = 8) and PD-1 KO mice (n = 8) in rotarod test, measured as latency to fall.

(F) Locomotor activity and anxiety-like behavior tests of WT mice (n = 10) and PD-1 KO mice (n = 10) in open field test.

(G) Anxiety-like behavior of WT mice (n = 10) and PD-1 KO mice (n = 10) measured by elevated-plus maze.

(H) Depressive-like behavior of WT mice (n = 10) and PD-1 KO mice (n = 10) measured by tail-suspension.

(I) MWM probe test for number of platform crossings in WT mice treated with control IgG (n = 12) and anti-mPD-1 mAb (n = 12).

(J) Swimming speed of WT mice treated with control IgG (n = 12) and anti-mPD-1 mAb (n = 12) in MWM probe tests.

(K) Cell-surface biotinylation and ELISA analysis showing membrane PD-1 levels in non-trained (n = 10) and trained (n = 10) mice.

(L) Flow cytometry gating strategy for PD-1^+ cells in hippocampal Vglut1^+ excitatory neurons.

Data are represented as mean ± SEM. $^{*}P < 0.05$, $^{**}P < 0.01$, $^{****}P < 0.0001$, ns: no significant. Two-tailed Student's t test (D, F, G, H, J, K), Two-way ANOVA (E), Mann-Whitney test (C, I).

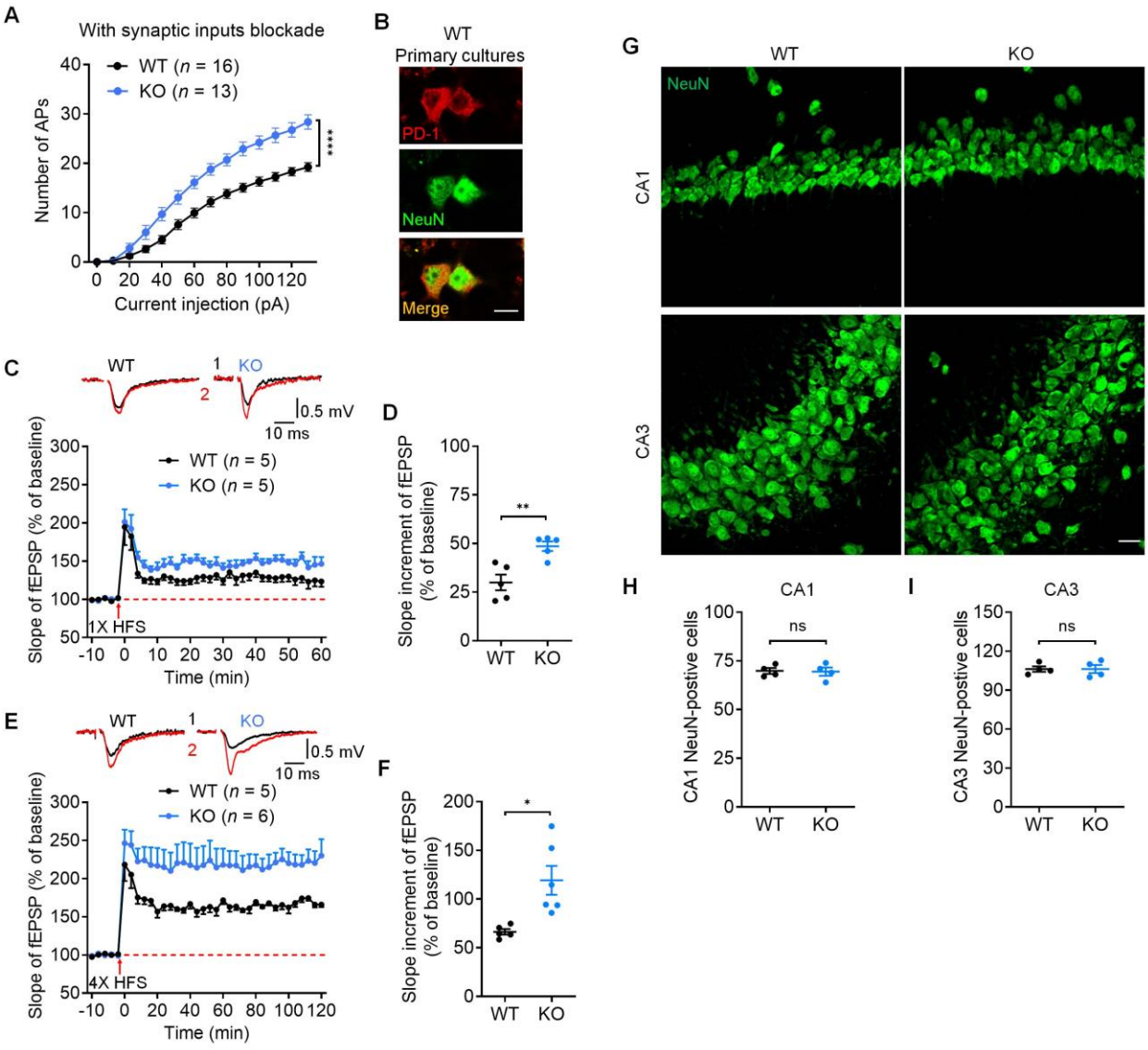

Figure S3. Characterization of electrophysiological parameters and neuronal numbers in mouse hippocampal neurons with PD-1 loss. Related to Figure 2 and Figure 3.

(A) Number of APs evoked by step current injection in WT and PD-1 KO CA1 neurons with synaptic input blockade. WT: *n* = 16 neurons from 4 mice; PD-1 KO: *n* = 13 neurons from 3 mice.

(B) Representative images of PD-1 immunocytochemistry in WT primary hippocampal neurons. Scale bar, 10 μm.

(C-F) LTP in the CA1 region of brain slices induced 1 × HFS and 4 × HFS.

(**C-D**) Summary plots (C) and average slope (D) of LTP induced by 1 × HFS in WT slices (*n* = 5 from 5 mice) and PD-1 KO slices (*n* = 5 from 5 mice). Top: Black traces (1) and red trace (2) represent the baseline fEPSP and post-induction fEPSP, respectively.

(**E-F**) Summary plots (E) and average slope (F) of LTP induced by 4 × HFS in the CA1 region of WT slices (*n* = 5 from 5 mice) and PD-1 KO slices (*n* = 6 from 5 mice). Top: Black traces (1) and red trace (2) represent the baseline fEPSP and post-induction fEPSP, respectively.
(G-I) Representative confocal microscopy images in CA1 and CA3 (G). Quantification of $NeuN^+$ neurons in CA1 (H) and CA3 (I) of WT mice and PD-1 KO mice (*n* = 4). Scale bar, 50 μm.

Data are represented as mean ± SEM. $^{*}P < 0.05$, $^{**}P < 0.01$, $^{****}P < 0.0001$, ns: no significant. Two-tailed Student's t-test (D, F, H, I), Two-way ANOVA (A).

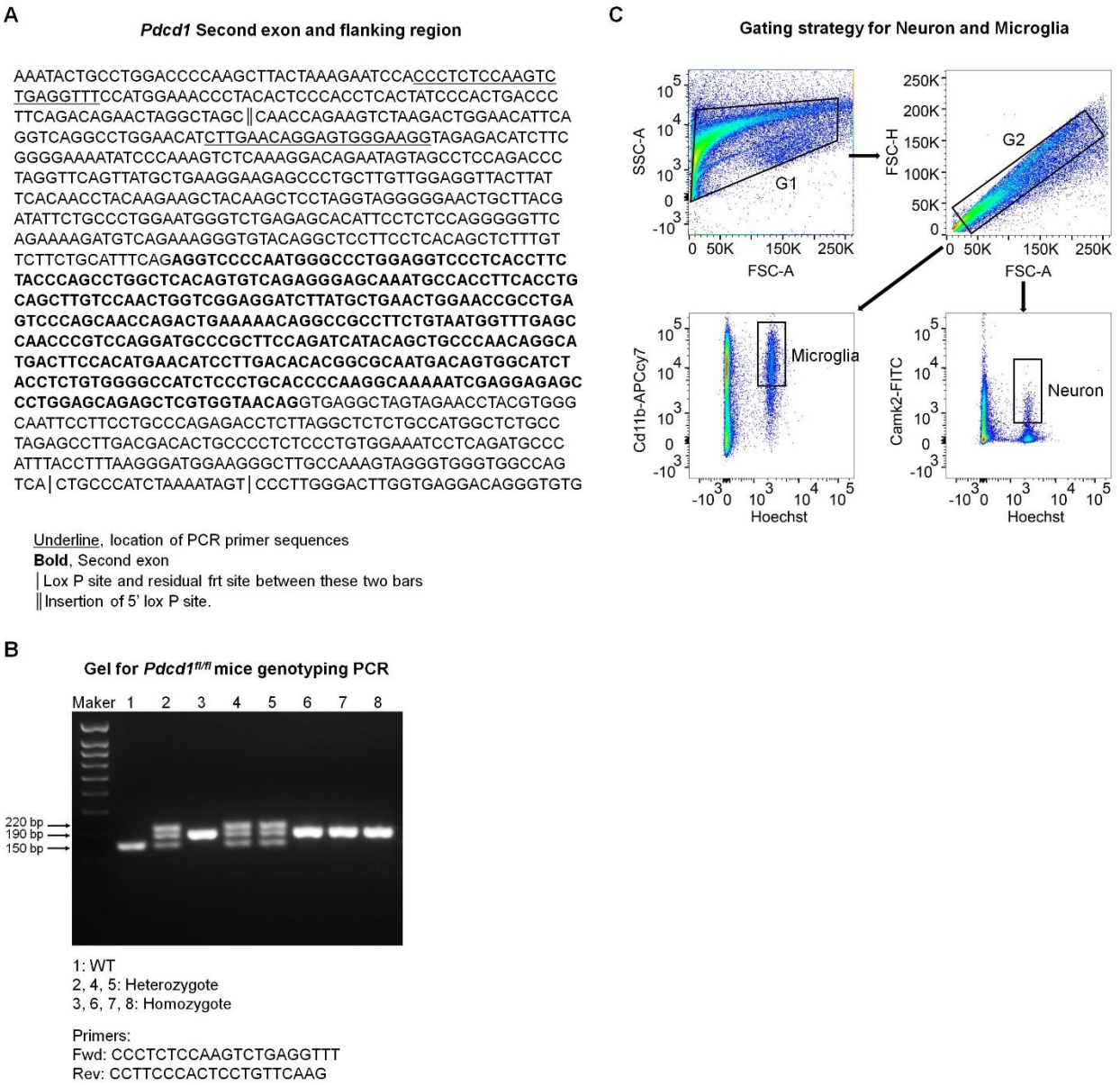

Figure S4. Schematic of generating *Pdcd1*$^{fl/fl}$ mice and validation of transgenic mice. Related to Figure 4.

(A) *Pdcd1* sequence including second exon (bold), Lox P site and residual frt site, and insertion of 5' lox P site. The sequences for the design of PCR primers are underlined.

(B) Validation of *Pdcd1*$^{fl/fl}$ mice via genotyping. Bottom, PCR primer sequences.

(C) Flow cytometry gating strategy for examining PD-1 expression in neurons and microglia.

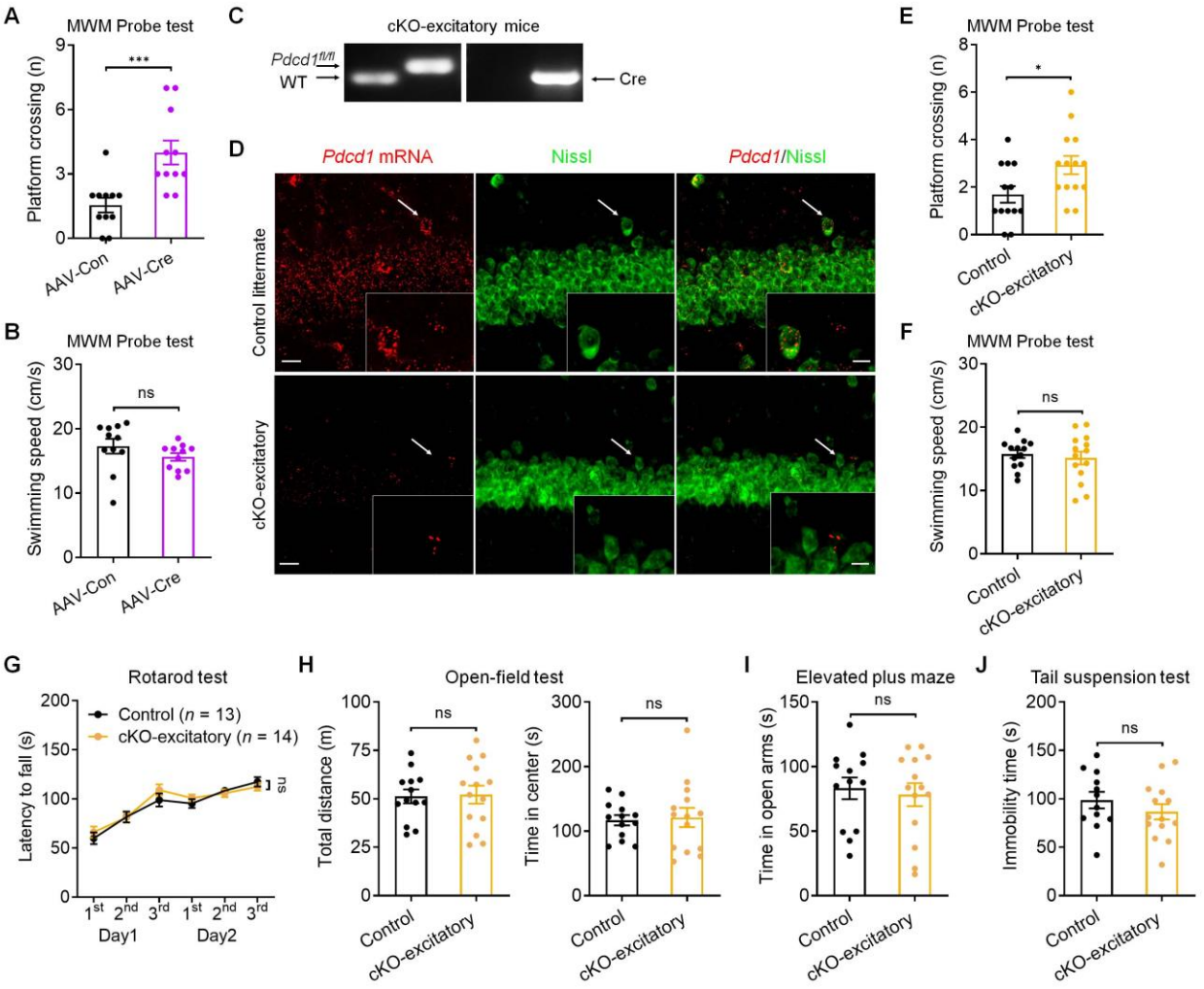

Figure S5. Conditional knockout of *Pdcd1* in excitatory neurons enhances learning and memory without altering emotional status. Related to Figure 4.

(A-B) MWM probe tests in *Pdcd1*$^{fl/fl}$ mice injected with AAV-control (n = 11) and AAV-*Camk2a*:Cre (n = 11) showing latency to platform (A) and swimming speed (B).

(C) Genotyping characterization of cKO-excitatory mice.

(D) Representative images show *Pdcd1* expression in CA1 neurons of control littermates, which is markedly reduced in cKO-excitatory mice. Scale bar, 20 μm. Inserted boxes are higher magnification images showing co-localization of *Pdcd1* with Nissl in CA1 neurons. Scale bar, 10 μm.

(E-F) MWM probe tests in control littermates (n = 13) and cKO-excitatory mice (n = 14) showing latency to platform (E) and swimming speed (F).

(G) Motor coordination of control littermates (n = 13) and cKO-excitatory mice (n = 14) in rotarod test.

(H) Locomotor activity and anxiety-like behavior of control littermates (n = 13) and cKO-excitatory mice (n = 14) in open-field test.

(**I)** Anxiety-like behavior of control littermates (n = 13) and cKO-excitatory mice (n = 14) in elevated-plus maze test.

(J) Depressive-like behavior of control littermates (n = 12) and cKO-excitatory mice (n = 14) in tail-suspension test.

Data are represented as mean ± SEM. $^{*}P < 0.05$, $^{***}P < 0.001$, ns: no significant. Mann-Whitney test (A, E), Two-tailed unpaired Student's t-test (B, F, H, I, J), Two-way ANOVA (G).

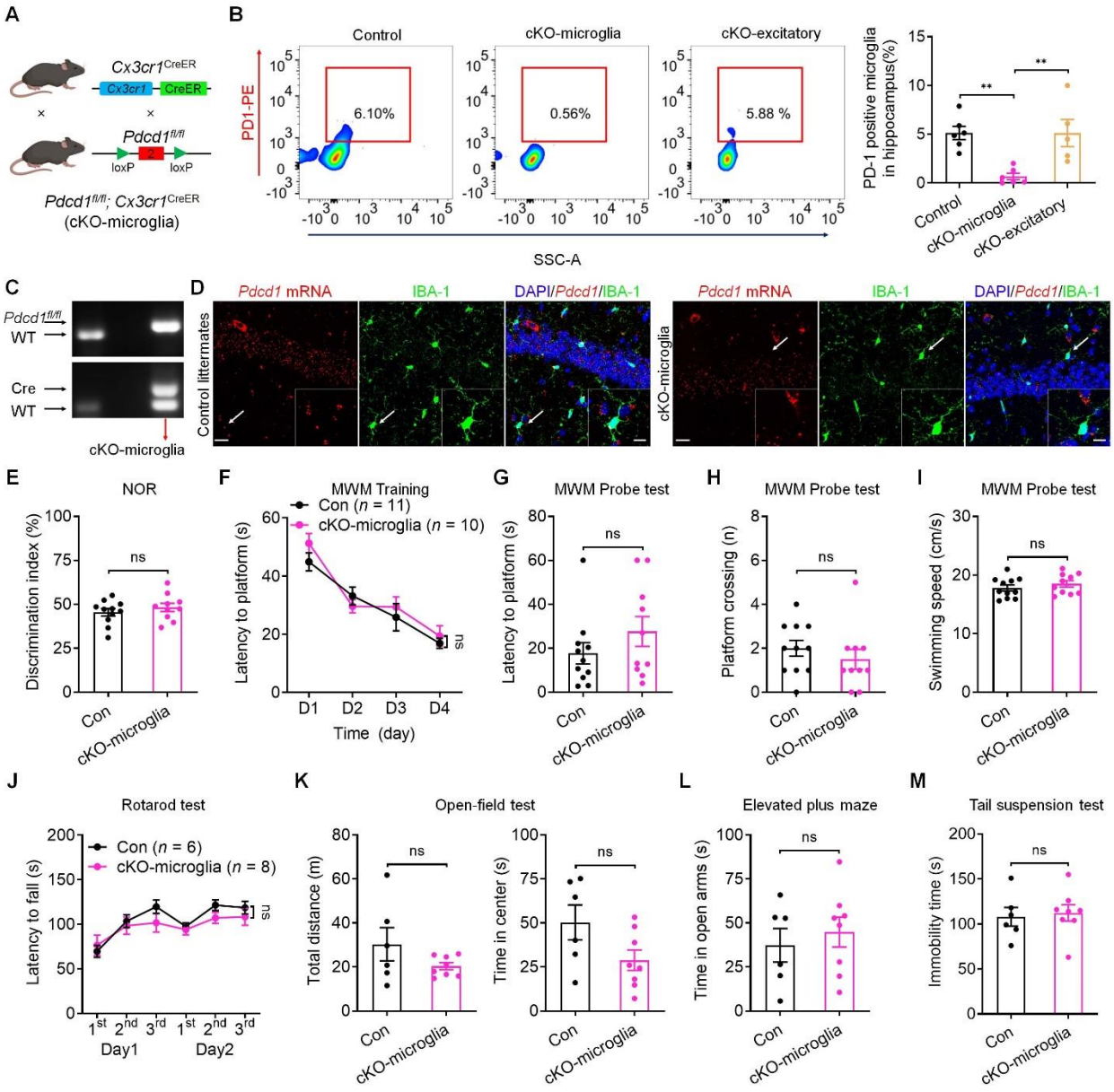

Figure S6. Conditional knockout of *Pdcd1* in microglia does not affect learning and memory. Related to Figure 4.

(A) Schematic illustration of the strategy to delete *Pdcd1* in microglia in conditional knockout mice (cKO-microglia).

(B) Flow cytometry images show the percentage of PD-1^{+} microglia in the hippocampi of control littermates (n = 6), cKO-microglia mice (n = 6), and cKO-excitatroy mice (n = 5). Note that PD-1 is lost in Cx3cr1^{+} microglia in cKO-microglia mice but not in control littermates or cKO-excitatory mice.

(C) Genotyping characterization of cKO-microglia mice.

(D) Representative images show *Pdcd1* expression in CA1 microglia of control littermates, which is substantially reduced in cKO-microglia mice. Scale bar, 20 μm. Inserted boxes are higher magnification images showing co-localization of *Pdcd1* with IBA-1 in CA1 neurons. Scale bar, 10 μm.

(E) Discrimination index of control littermates (n = 11) and cKO-microglia mice (n = 10) in NOR testing.

(F) Spatial learning curves during MWM training show learning capacity in control littermates (n = 11) and cKO-microglia mice (n = 10).

(G-I) MWM probe tests for latency to platform (G), platform zone crossings number (H), and swimming speed (I) in control littermates (n = 11) and cKO-microglia mice (n = 10).

(J) Motor coordination of control littermates (n = 6) and cKO-microglia mice (n = 8) in rotarod test.

(K) Locomotor activity (left) and anxiety-like behavior (right) in control littermates (n = 6) and cKO-microglia mice (n = 8) in open-field test.

(L) Anxiety-like behavior in control littermates (n = 6) and cKO-microglia mice (n = 8) measured in elevated-plus maze test.

(M) Depression-like behavior in control littermates (n = 6) and cKO-microglia mice (n = 8) measured in tail-suspension test.

Data are represented as mean ± SEM. $^{**}P < 0.01$, ns: no significant. One-way ANOVA with Tukey's post-hoc test (B), Two-tailed unpaired Student's t-test (E, I, K, L, M), Two-way ANOVA (F), Mann-Whitney test (G, H).

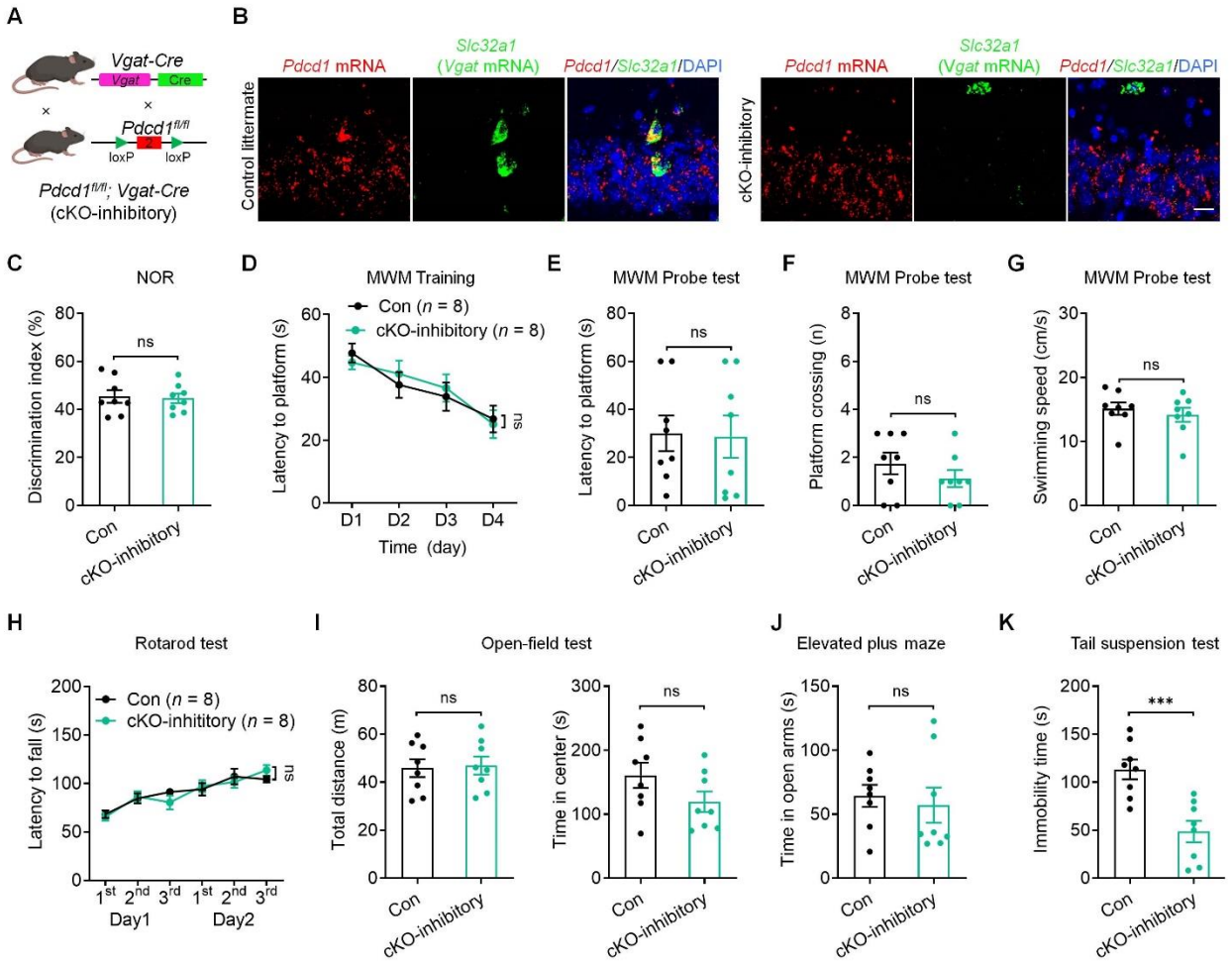

Figure S7. Conditional knockout of *Pdcd1* in inhibitory interneurons does not affect learning and memory. Related to Figure 4.

(A) Schematic illustration of the strategy to delete *Pdcd1* in inhibitory interneurons in conditional knockout mice (cKO-inhibitory).

(B) Representative images showing *Pdcd1* expression in CA1 inhibitory neurons of control littermates, which is substantially reduced in cKO-inhibitory mice. Scale bar, 20 μm.

(C) Discrimination index of control littermates (n = 8) and cKO-inhibitory mice (n = 8) in NOR test.

(D) Spatial learning curves during MWM training showing learning capacity in control littermates (n = 8) and cKO-inhibitory mice (n = 8).

(E-G) MWM probe tests for latency to platform (E), platform zone crossings number (F), and swimming speed (G) in control littermates (n = 8) and cKO-inhibitory mice (n = 8).

(H) Motor coordination of control littermates (n = 8) and cKO-inhibitory mice (n = 8) in rotarod test.

(I) Locomotor activity (left) and anxiety-like behavior (right) in control littermates (n = 8) and cKO-inhibitory mice (n = 8) in open-field test.

(J) Anxiety-like behavior in control littermates (n = 8) and cKO-inhibitory mice (n = 8) measured in elevated-plus maze test.

(K) Depression-like behavior in control littermates (n = 8) and cKO-inhibitory mice (n = 8) measured in tail-suspension test.

Data are represented as mean ± SEM. $^{***}P < 0.001$; ns, no significant. Two-tailed Student's t-test (C, G, I, J, K), Two-way ANOVA (D, H), Mann-Whitney test (E, F).

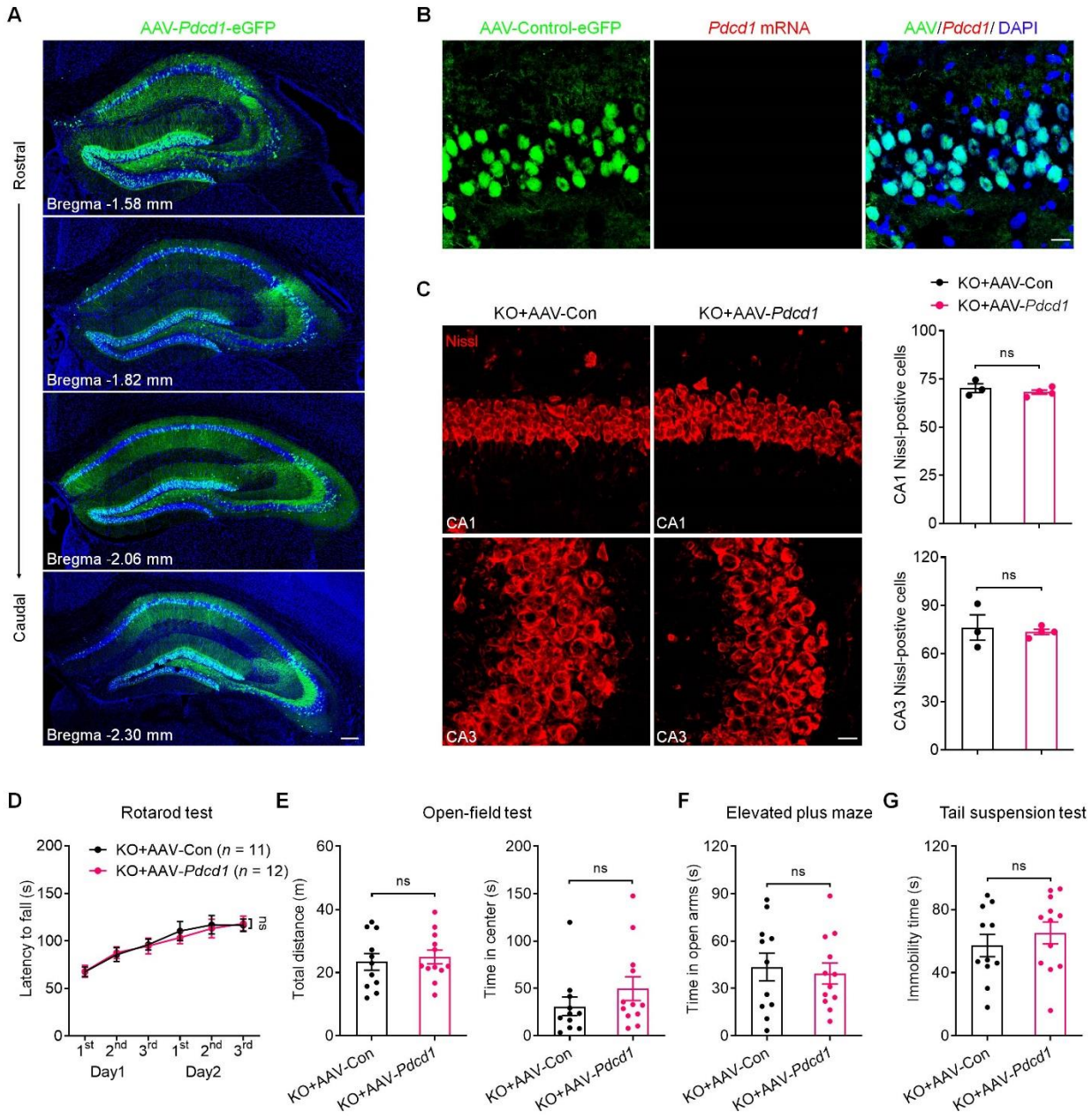

Figure S8. Characterization of *Pdcd1* expression, neuronal loss, and learning/memory behaviors in PD-1 KO mice following the AAV-*Pdcd1* injections into the hippocampus. Related to Figure 5.

(A) Representative confocal images of brain sections (rostral to caudal orientation) from mice injected with AAV-*Pdcd1* virus. Note extensive PD-1 expression (eGFP^{+}) in the hippocampus. Blue: DAPI staining. Scale bar, 200 μm.

(B) Representative confocal images showing no *Pdcd1* expression in PD-1 KO mice injected with AAV-control virus. Scale bar, 20 μm.

(C) Representative confocal images (left) and quantification of CA1 and CA3 neurons (right) in PD-1 KO mice injected with AAV-control (*n* = 3) and AAV-*Pdcd1* (*n* = 4). Note that AAV-*Pdcd1* treatment does not change neuron number in CA1 and CA3. Scale bar, 20 μm

(D) Motor coordination of in PD-1 KO mice injected with AAV-control (*n* = 11) and AAV-*Pdcd1* (*n* = 12) in rotarod test.

(E) Locomotor function (left) and anxiety-like behavior (right) in PD-1 KO mice injected with AAV-control (*n* = 11) and AAV-*Pdcd1* (*n* = 12) in open-field test.

(F) Anxiety-like behavior of PD-1 KO mice injected with AAV-control (*n* = 11) and AAV-*Pdcd1* (*n* = 12) measured by elevated-plus maze test.

(G) Tail suspension test in PD-1 KO mice injected with AAV-control (*n* = 11) and AAV-*Pdcd1* (*n* = 12) to measure depressive level.

Data are represented as mean ± SEM. ns: no significant. Two-tailed Student's t test (C, E, F, G, H), Two-way ANOVA (D).

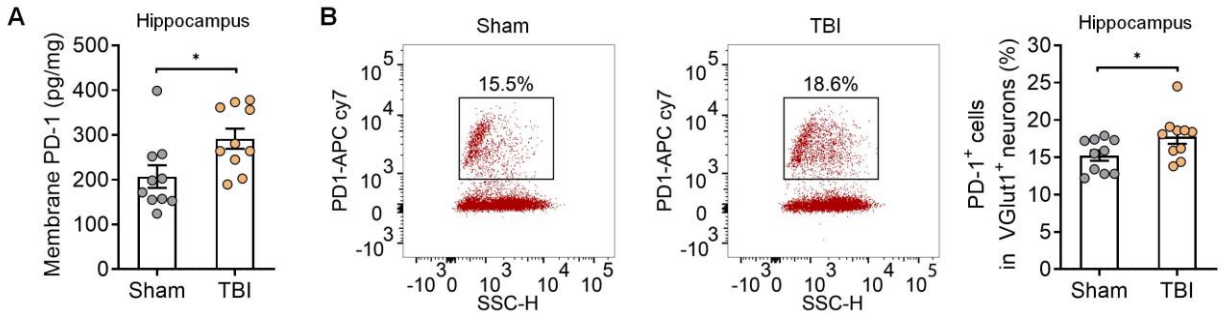

Figure S9. Membrane PD-1 expression in hippocampi from sham and TBI mice. Related to Figure 6.

(A) Cell-surface biotinylation and ELISA analysis showing membrane PD-1 levels in sham (n = 10) and TBI (n = 10) mice.

(B) Flow cytometry images (left) and quantification (right) showing the percentage of PD-1$^+$ cells in hippocampal Vglut1$^+$ excitatory neurons from sham (n = 10) and TBI mice (n = 10).

Data are represented as mean ± SEM. $^*P < 0.05$. Two-tailed Student's t test (A, B).

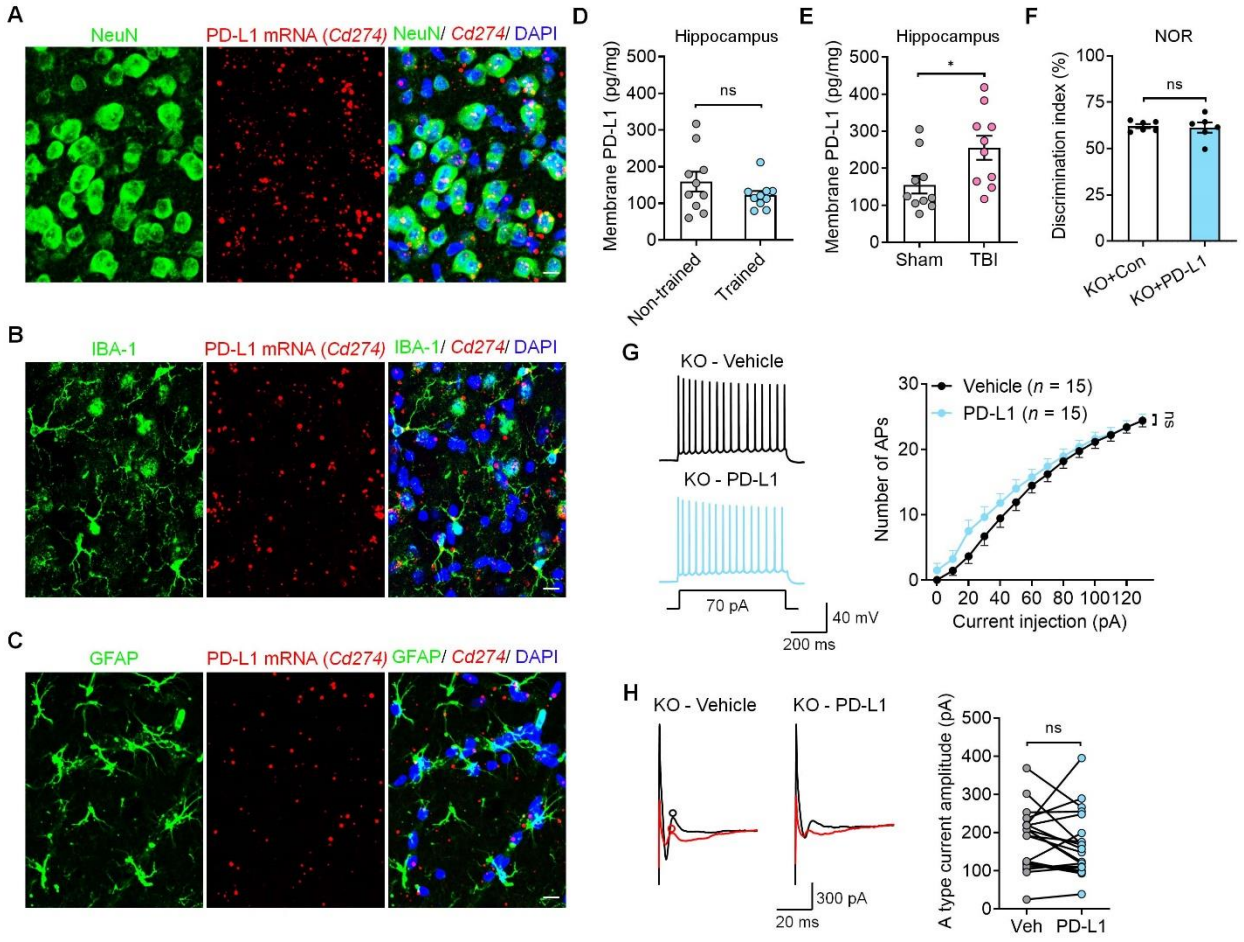

Figure S10. Characterization of PD-L1 (*Cd274*) expression, membrane PD-L1 level, and the effect of PD-L1 in PD-1 KO mice. Related to Figure 7.

(A-C) Representative confocal images showing double staining of *Cd274* mRNA (PD-L1, revealed by RNAscope) with NeuN (A), IBA-1 (B), GFAP (C). Scale bar, 20 μm.

(D) Cell-surface biotinylation and ELISA analysis showing membrane PD-L1 levels in non-trained (n = 10) and trained (n = 10) mice.

(E) Cell-surface biotinylation and ELISA analysis showing membrane PD-L1 levels in sham (n = 10) and TBI (n = 10) mice.

(F) Discrimination index of PD-1 KO mice treated with ICV injection of control (n = 6) or recombinant mouse PD-L1 (n = 6) in NOR testing.

(G) Representative AP traces (left) and number of APs evoked by step current injection (0-130 pA, 10 pA) (right) in CA1 neurons from PD-1 KO neurons before or after perfusion of recombinant mouse PD-L1 (50 ng/mL, n = 15 neurons from 4 mice).

(H) A type K^+ currents in CA1 neurons of brain slices of WT and PD-1 KO slices and the effects of PD-L1 (50 ng/mL). Left, representative outward current traces. Right, quantification of current amplitude before and after recombinant mouse PD-L1 perfusion (n = 21 neurons from 4 mice). Black trace: nonconditioned current; red trace: conditioned current. A type current was isolated from the subtraction of red to black circles.

Data are represented as mean ± SEM. $^{*}P < 0.05$. ns, not significant. Two-tailed Student's t-test (D, E, F), Two-way ANOVA (G), Two-tailed paired Student's t-test (H).

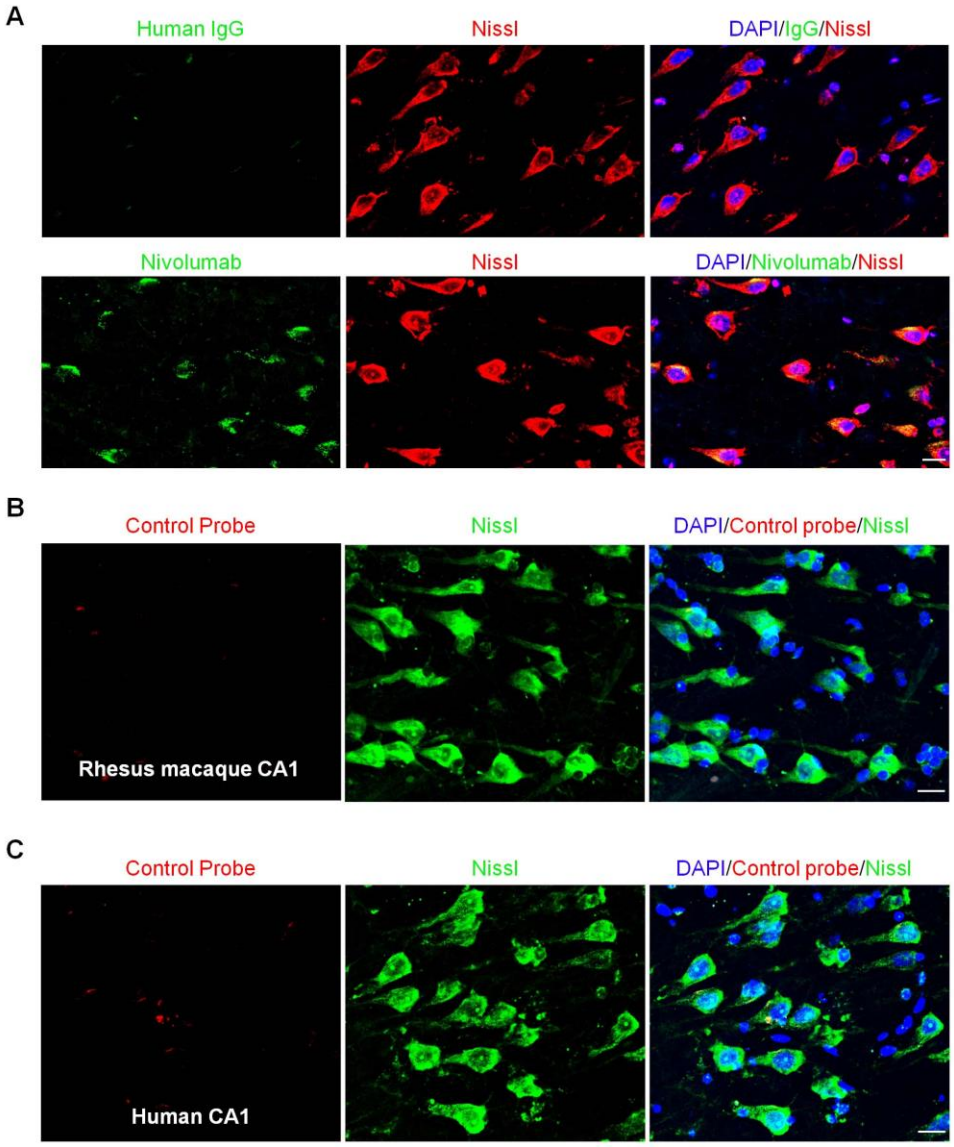

Figure S11. Validation of *PDCD1* expression in NHP and human hippocampal neurons. Related to Figure 8.

(A) Representative images showing nivolumab (anti-human PD-1 mAb) but not human IgG binding to human CA1 neurons. Scale bar, 20 μm.

(B-C) Representative images of *in situ* hybridization show no staining of negative control probe in hippocampal neurons of NHP (B) and human (C) brain sections. Scale bar, 20 μm.

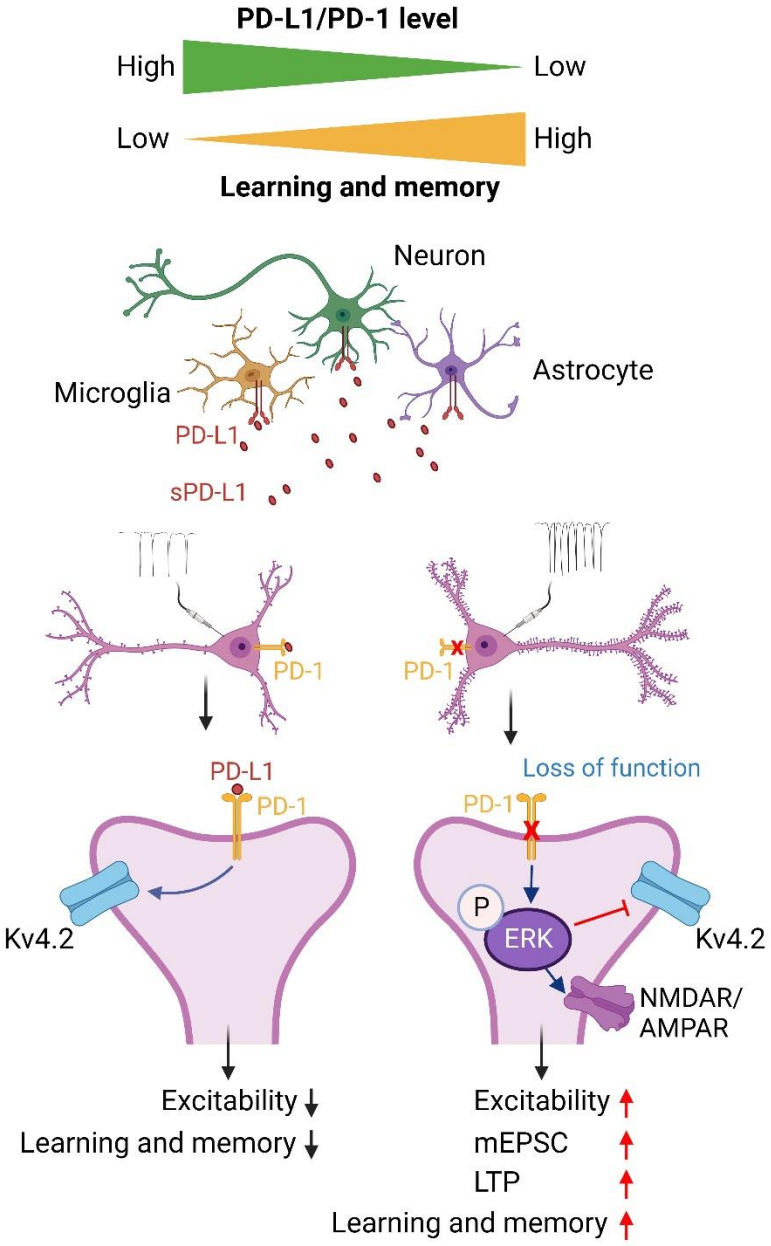

Figure S12. Schematic of the working hypothesis for the regulation of neuronal excitability, synaptic transmission, and cognition by the PD-L1/PD-1 checkpoint pathway.

Table S1. Number of mice and samples used in this study. Related to Figures 1-8.

(note: mice shared in different experiments are underlined.)

Provided as a separate Excel file.

Table S2. Information for human donors/participants in this study, Related to Figures 7-8 and STAR Methods.

Human	Sex	Ages	Sample collection and experiments
H1	Female	59 years old	Hippocampi collection for RNAscope
H2	Male	60 years old	Hippocampi collection for RNAscope
H3	Female	49 years old	Plasma/CSF collection for ELISA
H4	Female	22 years old	Plasma/CSF collection for ELISA
H5	Female	46 years old	Plasma/CSF collection for ELISA
H6	Female	69 years old	Plasma/CSF collection for ELISA
H7	Female	62 years old	Plasma/CSF collection for ELISA
H8	Female	37 years old	Plasma/CSF collection for ELISA
H9	Female	44 years old	Plasma/CSF collection for ELISA
H10	Male	64 years old	Plasma/CSF collection for ELISA

Table S3. Information for NHPs used in different experiments in this study, Related to Figures 7-8 and STAR Methods.

NHP	Sex	Ages	Sample collection and experiments
MK1	Male	17 years old	CSF collection before and after capsaicin injection for ELISA
MK2	Male	10 years old	CSF collection before and after capsaicin injection for ELISA
MK3	Female	20 years old	CSF collection before and after capsaicin injection for ELISA
MK4	Female	10 years old	Serum collection before capsaicin injection for ELISA CSF collection before and after capsaicin injection for ELISA
MK5	Female	10 years old	Serum collection before capsaicin injection for ELISA CSF collection before and after capsaicin injection for ELISA
MK6	Female	9 years old	Serum collection before capsaicin injection for ELISA CSF collection before and after capsaicin injection for ELISA
MK7	Male	7 years old	Serum collection before capsaicin injection for ELISA CSF collection before and after capsaicin injection for ELISA
MK8	Female	13 years old	Hippocampi collection for electrophysiology and RNAscope
MK9	Male	19 years old	Hippocampi collection for electrophysiology and RNAscope
MK10	Female	10 years old	Hippocampi collection for electrophysiology and RNAscope
MK11	Male	9 years old	Hippocampi collection for electrophysiology
MK12	Female	11 years old	Hippocampi collection for electrophysiology
MK13	Male	23 years old	Hippocampi collection for electrophysiology

Table S4. Sequences of PCR primers for mouse genotyping experiments, Related to STAR Methods.

Mouse line	Source	Primer direction	Sequences
Pdcd1$^{-/-}$	The Jackson Laboratory	Common Forward	CACTATCCCACTGACCCTTCA
		Wild type Reverse	AGAAGGTGAGGGACCTCCAG
		Mutant Reverse	CACAGGGTAGGCATGTAGCA
Pdcd1$^{fl/fl}$	This paper	Forward	CCCTCTCCAAGTCTGAGGTTT
		Reverse	CCTTCCCACTCCTGTTCAAG
Camk2a-Cre	The Jackson Laboratory	Forward	TTACCGGTCGATGCAACGAGT
		Reverse	TTCCATGAGTGAACGAACCTGG
Cx3cr1^{CreER}	The Jackson Laboratory	Common Forward	ACGCCCAGACTAATGGTGAC
		Wild type Reverse	AGCTCACGACTGCCTTCTTC
		Mutant Reverse	GTTAATGACCTGCAGCCAAG
Vgat-Cre	The Jackson Laboratory	Common Forward	CTTCGTCATCGGCGGCATCTG
		Wild type Reverse	CAGGGCGATGTGGAATAGAAA
		Mutant Reverse	CCAAAAGACGGCAATATGGT
Ai9	The Jackson Laboratory	Wild type Forward	AAGGGAGCTGCAGTGGAGTA
		Wild type Reverse	CCGAAAATCTGTGGGAAGTC
		Mutant Forward	CTGTTCCTGTACGGCATGG
		Mutant Reverse	GGCATTAAAGCAGCGTATCC
Pdcd1-Cre	This paper	Forward	CCAGGCCCCCAGAGCCATATC
		Reverse	CCATAGGCTCCCCATTGACTTCTTG

Table S5. Statistical table. Related to Figures 1-8.

Provided as a separate Excel file.